RSC Advances

ROYAL SOCIETY OF CHEMISTRY

www.rsc.org/advances

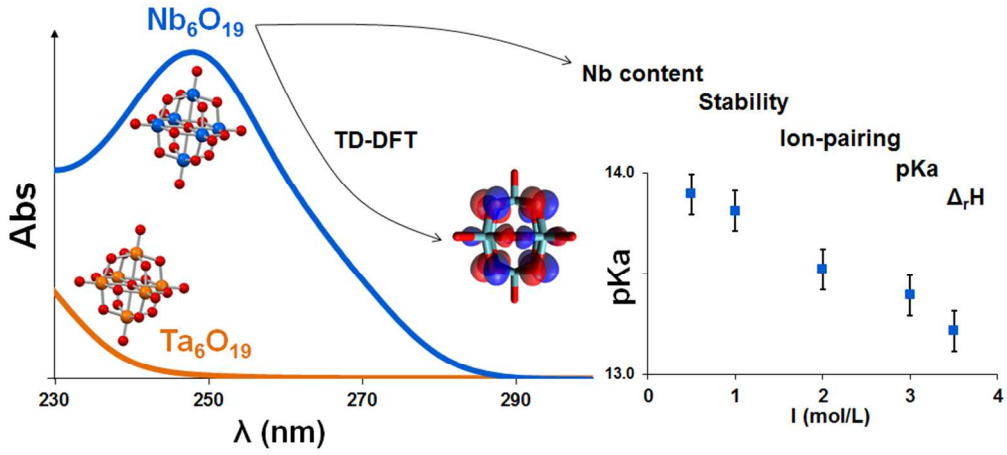

274x123mm (96 x 96 DPI)

RSC Advances

RSCPublishing

ARTICLE

Experimental and computational exploration of the UV-visible properties of hexaniobate and hexatantalate ions

Cite this: DOI: 10.1039/x0xx00000x

Received 00th month 201X,
Accepted 00th month 201X

DOI: 10.1039/x0xx00000x

www.rsc.org/

Gauthier J-P. Deblonde,*[a,b] Aurélien Moncomble,[c] Gérard Cote,[a] Sarah Bélair[b] and Alexandre Chagnes[a]

The UV-visible properties of hexaniobate ($H_xNb_6O_{19}^{x-8}$) and hexatantalate ($H_xTa_6O_{19}^{x-8}$) ions were investigated experimentally and by DFT calculations. Due to the huge discrepancies among the reported values found in prior studies, the extinction coefficients of hexaniobate ions were determined from multiple samples in various media. A simple and low-cost method was then developed for the determination of the niobium content of both synthetic and industrial samples. Taking advantage of the UV spectra of the hexaniobate ions, the first protonation constant of $Nb_6O_{19}^{8-}$ could be determined experimentally (pKa = 13.4 ± 0.1 at 25 °C, Δ_rH = -95 kJ/mol in 3 M KOH/KCl) and is in accordance with the reported values previously extrapolated from potentiometric measurements (pKa= 13.3 ± 0.6). UV batch titrations performed at different ionic strengths suggest that the equilibrium between the monoprotonated and the deprotonated forms of the Lindqvist ion is accompanied by an exchange of potassium ions and that the cluster is easier to deprotonate in Na^+ media. This study highlights the importance of the ion-pairing on the chemistry of these polyoxometalates. The tremendous difference between the UV spectrum of $Nb_6O_{19}^{8-}$ and $Ta_6O_{19}^{8-}$ was investigated by DFT computations. The UV spectra were reproduced and show a good agreement with the experimental data. Moreover this study allowed to give some insights in the evolution of the spectra together with the pH of the medium by studying the nature of the transitions involved in this spectral domain.

Introduction

Niobium (Z= 41) and tantalum (Z= 73) are catching growing attention because they play a critical role in alloys and electronic industries. However, the development of efficient, economic and environmentally friendly processes to recover them from ores is still a challenge. Although classical routes to recover and purify niobium and tantalum require highly acidic and fluoride containing solutions[1], the chemistry of both valuable metals has been extensively studied in alkaline media over the past decades. Indeed, high solubility of Nb(V) and Ta(V) can be reached in alkaline solutions along with separation from impurities such as Fe, Mn and Ti.[2] The chemistry of Nb(V) and Ta(V) at basic pH is dominated by the Lindqvist type ions $H_xM_6O_{19}^{x-8}$ (M= Nb, Ta ; $0 \leq x \leq 3$).[3] The structure of the cluster M_6O_{19} has been widely investigated and consists of a super octahedron of six edge-sharing octahedra MO_6 yielding three different types of oxygen atoms: one central atom μ_6–O, six terminal oxygens η–O and twelve bridging oxygens μ_2–O (Fig. 1).

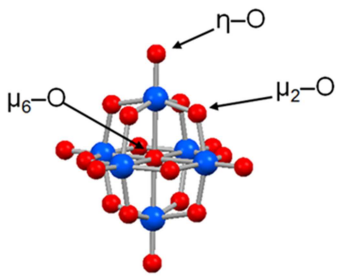

Fig. 1 Ball-and-stick representation of the Lindqvist ion M_6O_{19} (Red: oxygens. Blue: niobium or tantalum) which contains 1 central oxygen (μ_6–O), 6 terminal oxygens (η–O) and 12 bridging oxygens (μ_2–O).

Contrasting with the renewed interest in alkaline solutions of Nb and Ta, methods to determine niobium and tantalum content in alkaline samples are still limited to Inductively Coupled Plasma spectrometry. In this regard, the UV-visible properties of the hexaniobate and hexatantalate ions could help to implement new and cheap methods for the determination of Nb

and Ta content in samples. UV-based methods could also be developed to probe the solution thermodynamics of $H_xM_6O_{19}^{x-8}$ ions, including pKa determination and stability of these polyoxometalates. Surprisingly, the studies published on the absorbance properties of hexaniobate and hexatantalate ions are scarce and took place in the early development of polyoxoniobates and polyoxotantalates chemistry when the existence of the hexameric species was still controversial. In the early 60's, Jander and Ertel[4] first performed a spectrophotometric study on hexaniobate ions showing a strong absorbance band below 300 nm with a maximum lying between 250 and 230 nm depending on the pH. The only hexatantalate UV spectrum was reported three years later by Nelson and Tobias[5] highlighting the low absorbance properties of $H_xTa_6O_{19}^{x-8}$ ions compared to their niobium counterparts. Knowing that Nb(V) and Ta(V) have identical ionic radii[6] and very similar electronic configurations, resulting in quasi-identical geometry for Nb_6O_{19} and Ta_6O_{19} clusters,[7] the striking difference between their UV properties challenges our understanding and needed to be investigated.

The present study revisits the UV properties of hexaniobate and hexatantalate ions. The absorbance properties of hexaniobate ions allowed us to implement a fast and convenient method for the determination of Nb concentration in various samples including those found in industrial processes used for Nb and Ta recovery. Taking advantage of the UV absorbance of hexaniobate ions, the first protonation constant and its reaction enthalpy have been determined experimentally for the first time. Finally, the tremendous difference between the UV properties of Nb and Ta Lindqvist ions has been investigated by DFT calculations and enriches our understanding on Nb and Ta chemistry in alkaline media.

Experimental section and computational details

Regents. All stock solutions were prepared with deionized water (R> 18.2*10^6 Ω) degassed by boiling for 1 h while being purged under N_2. All stock solutions were kept in a glove box under N_2 atmosphere. Nb_2O_5 99.9% (Sigma Aldrich), $Nb(HC_2O_4)_5$,nH_2O (Alfa Aesar, 19.2 w% Nb) and $NbCl_5$ 99% (Alfa Aesar) were used without further purification. Industrial alkaline solutions of Nb(V) were provided by Eramet Research company (France). These samples were slightly contaminated by Ta(V); Nb/Ta= 80 mol/mol. Stock solutions of NaCl (VWR), KCl (VWR), CsOH,H_2O (Alfa Aesar) and potassium hydrogen phthalate (99.98%, Fluka) were obtained by direct dissolution of weighed samples in CO_2-free deionized water. The KOH stock solution was purchased and opened under N_2 atmosphere (Alfa Aesar, Selectipur®, 30 w% KOH. An analytical certificate provided by the manufacturer gives a CO_2 contamination of 0.3 w% K_2CO_3). The concentrated KOH stock solution was standardized by titrating against potassium hydrogen phthalate under positive N_2 pressure. The titration was repeated four times and yielded a KOH concentration of 6.761 ± 0.020 mol/L. The NaOH stock solution was prepared by dissolving NaOH pellets in CO_2-free deionized water. The NaOH solution was further purged with N_2 for 1 h and titrated against potassium hydrogen phthalate ([NaOH] = 4.866 ± 0.020 mol/L). For the synthesis of $K_8Nb_6O_{19}$,$16H_2O$, $NbCl_5$ was hydrolyzed at pH 4 to produce Nb_2O_5,nH_2O which was then used to produce the potassium hexaniobate salt as reported by Nyman et al.[8] $K_8Nb_6O_{19}$,$16H_2O$ was identified by powder XRD (ICDD PDF 01-077-4938), Raman spectroscopy and thermogravimetric analysis (TGA). Raman (cm^{-1}): 875 ; 827 ; 745 ; 529 ; 460 ; 376 ; 288 ; 217. TGA: %H_2O found = 19.6 w% (theoretical: 19.7). $Na_7HNb_6O_{19}$,$15H_2O$ was synthesized by alkaline fusion (5h at 450°C, NaOH/Nb_2O_5 = 10 mol/mol), washed and recrystallized in water. The product was also identified by powder XRD (ICDD PDF 04-016-4410), Raman spectroscopy and TGA. Raman (cm^{-1}): 904 ; 837 ; 769 ; 524 ; 485 ; 458 ; 380 ; 278 ; 215 ; 172. TGA: %H_2O found = 21.5 w% (theoretical: 20.9).

Materials. A Vista Pro spectrometer (Varian) was used for ICP-AES titrations. Quantitative analyses were performed at 295.088 nm spectral emission line for Nb. All UV spectra were measured on a Cary 100-Scan spectrometer used in double beam mode. Each spectrum was acquired in Quartz Suprasil® cuvette (path length of 10.00 mm) and recorded against the corresponding blank sample. The cuvette lixiviation in high alkaline media was checked to be very limited in order to avoid silicate contamination (provider's data: dissolution of 0.27 µg.cm^{-2}.h^{-1} with KOH 30 w%). The alkaline samples were hold in the cuvettes less than 5 min and then discarded.

UV batch titrations. Each acid-base titration contained, at least, 8 samples prepared under N_2 atmosphere by diluting the stock solutions of KCl, KOH and $K_8Nb_6O_{19}$,$16H_2O$ or NaCl, NaOH and $Na_7HNb_6O_{19}$,$15H_2O$ with CO_2-free deionized water. Polyethylene vessels were used to avoid contamination by silicates. The hydroxide concentration was varied from 0.01 mol/L to the maximum value (which equals the ionic strength of the series) while the niobium concentration and the ionic strength were kept constant. The total niobium concentration was typically 2.4*10^{-4} mol/L *i.e* $\Sigma[H_xNb_6O_{19}^{x-8}]$ = 4*10^{-5} mol/L. The corresponding blank samples were prepared similarly without niobium. After being thermostated under N_2 atmosphere for 24h, the UV spectrum (220-350 nm – 260 data points) of each sample was recorded against its corresponding blank.

Data treatment. For each batch titration, the UV spectra, the extinction coefficient of the deprotonated species, the total hexaniobate concentration and the estimated pH were imported into the refinement program HypSpec[9] and analyzed by nonlinear least-squares refinement. The determination of equilibrium constants by this software has proven its efficiency elsewhere.[10,11,12] The protonation constant given is this work refers to the following equation:

$$Nb_6O_{19\,(aq)}^{8-} + H_3O^+ = HNb_6O_{19\,(aq)}^{7-} + H_2O \qquad (1)$$

Due to the low concentration of hexaniobate compared to hydroxide ions in the samples ($[HNb_6O_{19}^{7-}] + [Nb_6O_{19}^{8-}] = 4*10^{-5}$ mol/L compared to $0.01 \leq [HO^-] \leq 3.00$ mol/L), the hydroxide concentration in each sample was evaluated from the volume of standardized stock solutions. The corresponding pH was calculated using equation (2).

$$pH = -\log\left(\frac{Kw}{[HO^-]}\right) \qquad (2)$$

The Kw values in KCl/KOH media at the different ionic strengths and temperatures were taken from Sweeton et al.[13] The Kw values in NaCl/NaOH media were taken from Kron et al.[14] The whole procedure (samples preparation, UV batch titration and data treatment) was duplicated for 3 different ionic strengths and 2 different temperatures so that the uncertainty of the method was determined to be ± 0.1 log unit.

Computational details. All calculations were carried out using DFT-based methods, and more specifically the PBE0 global hybrid functional.[15,16] The Gaussian 09 software was used throughout.[17] For optimizations, oxygen was represented by the Dunning basis set[18] while Nb and Ta were described by the Stuttgart-Dresden ECP and its associated basis set.[19] For thermodynamics and UV-vis properties, single points were processed on the optimized structured using the larger Def2-TZVP basis set for the three elements.[20] Optimizations were carried out without any symmetry constraint using standard algorithms and the nature of the minima was checked by vibrational analysis. The solvent was taken into account using an implicit model, namely the Polarizable Continuum Model (PCM)[21] as implemented in Gaussian 09.
Electronic transitions were computed in the time-dependent variant of DFT (TD-DFT) within the adiabatic approximation taking into account the 250 lowest-lying excited states. To produce spectra, each transition was convoluted using a Gaussian-centered function with a 3000 cm^{-1} FWHM and all components were added.

Results

UV properties of hexaniobate ions. The UV spectrum of hexaniobate solutions displays a large absorbance band below 300 nm with a maximum lying between 250 and 240 nm depending on the hydroxide concentration (Fig. 2). Upon increasing of the pH, the absorbance wavelength of the charge transfer band shifts from 241.5 nm in presence of 0.01 M of KOH to 247.5 nm in 3.00 M KOH. Measurements performed with a KOH concentration ranging from 3 M to 9 M did not show further variations of the UV spectra (Fig. 3 and Fig. S1). The red shift observed in the UV spectrum is characteristic of the deprotonation of the hexaniobate ion $HNb_6O_{19}^{7-}$ and suggests that a hydroxide concentration higher than 3 M is required to fully deprotonate the hexaniobate cluster. The isosbestic point observed at 240 nm indicates the presence of an equilibrium between the deprotonated and the monoprotonated clusters. Taking into account these observations, the extinction coefficient of the fully deprotonated cluster $Nb_6O_{19}^{8-}$ was determined experimentally.

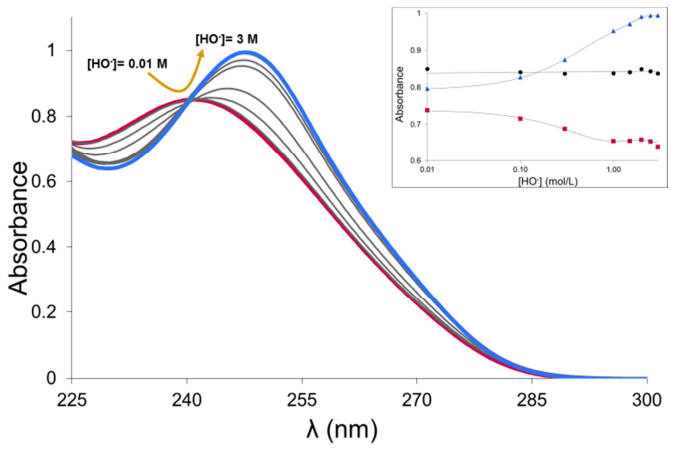

Fig. 2 UV spectra of hexaniobate solutions with hydroxide concentration varying from 0.01 M to 3.00 M. I = 3 M (KCl/KOH). T = 25 °C. $[Nb_6O_{19}]_{total} = 6.3*10^{-5}$ M. Path length = 10.00 mm. Inlet: Absorbance change at 247.5 nm (triangles), 240.0 nm (circles) and 230.0 nm (squares) with the corresponding HypSpec fits.

Due to huge discrepancy in the literature data[4,22,23], special care was taken in order to determine the molar absorptivity of $Nb_6O_{19}^{8-}$. More than thirty independent samples with various media (Fig. S2) were diluted in 4 M KOH, their UV spectrum was recorded and their niobium content was determined by conventional Inductively Coupled Plasma spectrometric titration (ICP-AES). The extinction coefficient ε_{Nb6O19}= 15,900 ± 600 L/mol/cm was determined for $Nb_6O_{19}^{8-}$. In order to validate this value, samples of niobium oxalate were prepared by dissolution of commercial $Nb(HC_2O_4)_5,nH_2O$ in water, the samples were then diluted in 4 M KOH and their UV spectra were recorded after 10 min equilibration time. The same procedure was implemented for solutions of commercial $NbCl_5$ dissolved in HCl. The Nb concentration of each sample was calculated using Beer-Lambert's law and the extinction coefficient value previously determined.

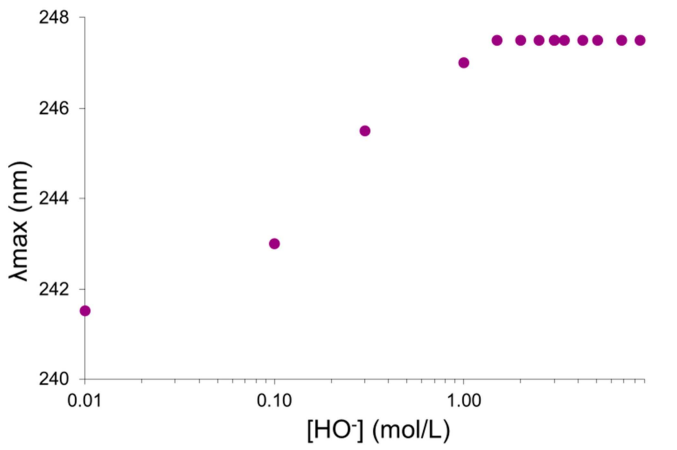

Fig. 3 Variation of the wavelength at maximal absorbance for $H_xNb_6O_{19}^{x-8}$ as a function of hydroxide concentration. I = 3 M (KCl/KOH) for samples with $[HO^-] \leq 3$ M. Ionic strength not maintained for samples with $[HO^-] > 3$ M. T = 25 °C. $[Nb_6O_{19}]_{total} = 6.3*10^{-5}$ M.

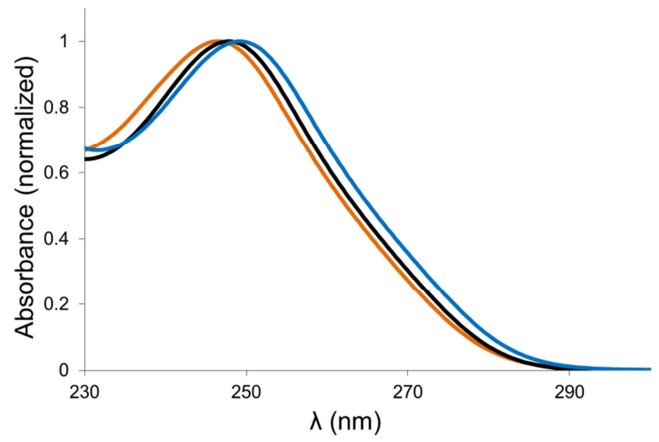

Fig. 4 Absorbance spectra of $Nb_6O_{19}^{8-}$ measured in 4 M NaOH (orange), 4 M KOH (black) and 4 M CsOH (blue).

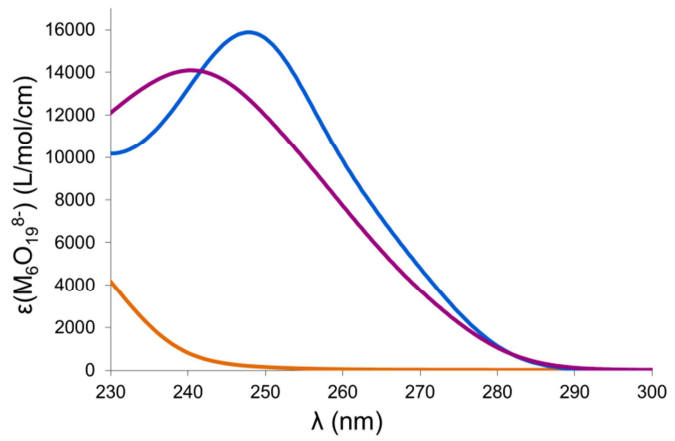

Fig. 5 Molar absorptivity of $Ta_6O_{19}^{8-}$ (orange) and $Nb_6O_{19}^{8-}$ (blue) determined experimentally and molar absorptivity of $HNb_6O_{19}^{7-}$ (purple) calculated from UV batch titrations.

The theoretical Nb concentrations and those obtained by the UV titration are in good agreement for both niobium chloride and niobium oxalate samples as displayed in Fig. S3. The UV-based method was also used to determine the Nb content of 17 independent industrial solutions of hexaniobate. The concentrations measured by UV titration and by ICP-AES are in good agreement (Fig. S4) confirming the value of 15,900 L/mol/cm ε_{Nb6O19}. The linear range of the method was found to be $5*10^{-6}$ to 10^{-4} M of $Nb_6O_{19}^{8-}$. The influence of the ionic media on the UV spectrum of $Nb_6O_{19}^{8-}$ was checked by diluting hexaniobate samples in 4 M NaOH, KOH and CsOH. The nature of the alkali ion does not influence the shape of the charge transfer band but the wavelength at maximum absorbance (λ_{max}) is slightly shifted from 246.5 in NaOH to 247.5 in KOH and 249 nm in CsOH (Fig. 4)

UV properties of hexatantalate ions. Compared to their niobium counterparts, solutions of hexatantalate ions $H_xTa_6O_{19}^{x-8}$ ($x \leq 3$) exhibit a relatively low absorbance in the UV region. Variation of the hydroxide concentration from 0.01 M to 9 M has no influence on the UV spectra suggesting that the hexatantalate ion is fully deprotonated at pH ≥ 12. At 247.5 nm, which is the wavelength of maximum absorbance for $Nb_6O_{19}^{8-}$, the molar absorptivity of $Ta_6O_{19}^{8-}$ is 80 times lower than that of its niobium equivalent (Fig. 5). At the isosbestic point of 240 nm observed for hexaniobate, the ratio $\varepsilon_{Nb6O19}/\varepsilon_{Ta6O19}$ is still 20.

pKa determination. The variation observed on the hexaniobate UV spectrum while varying the hydroxide concentration was large enough to accurately determine equilibrium constant. Nonlinear least-squares fits of the spectra included the fully deprotonated species $Nb_6O_{19}^{8-}$ and the monoprotonated species $HNb_6O_{19}^{7-}$ (Fig. 5). The refinement process also enabled us to determine the extinction coefficient of the monoprotonated species $HNb_6O_{19}^{7-}$.

Spectrophotometric batch titrations were performed in KOH/KCl and NaOH/NaCl media at different ionic strengths and temperatures. The equilibrium constant decreases when the ionic strength increases. At a given ionic strength and temperature the pKa $HNb_6O_{19}^{7-}/Nb_6O_{19}^{8-}$ was found to be lower in NaCl/NaOH media than in KCl/KOH media. The results are summarized in Fig. 6.

For an ionic strength of 3 M (KOH/KCl), the equilibrium constant was determined at different temperatures (Fig. 7). The refinement of the titration data showed that the reaction is exothermic. Using Van't Hoff's equation, the reaction enthalpy was determined and yielded a Δ_rH value of -95.1 kJ per mole of hexaniobate.

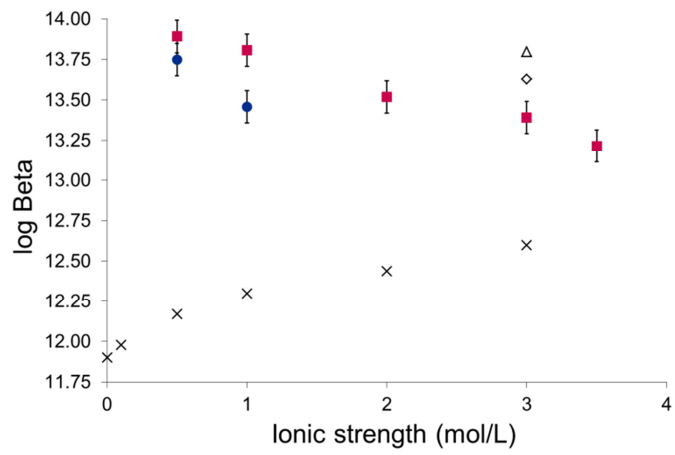

Fig. 6 Protonation constant of $Nb_6O_{19}^{8-}$ measured at 25 °C in KCl/KOH media (square) and NaCl/NaOH media (circle) and values extrapolated by Neuman[24] (triangle), Spinner et al.[25] (crosses) and Etxebarria et al.[26] (lozenge). The error bars correspond to ± 0.1 log unit.

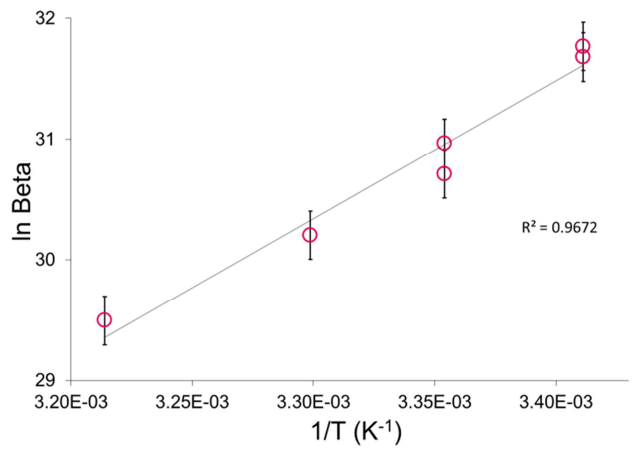

Fig. 7 Effect of temperature on the protonation constant of $Nb_6O_{19}^{8-}$. I = 3 M (KCl/KOH). The error bars correspond to ± 0.1 log unit.

Discussion

Even though hexaniobate and hexatantalate ions have been known for a long time[4,5], their UV-vis properties are still poorly investigated. To our knowledge, the only published data mentioning the UV properties of Nb and Ta Lindqvist ions are graphical.[5,23,24,22,27] Extrapolation of the molar absorption coefficient from these pioneer studies revealed a huge discrepancy as shown in Table 1. Thus, a precise determination of the extinction coefficients was needed in order to develop UV-based methods for probing the hexaniobate and hexatantalate solution thermodynamics. The strong discrepancy between literature data is surprising but might be imputable to the titration methods used for niobium at the time like ignition and weighting of the sample as Nb_2O_5 which can be easily biased in presence of alkali ions (A) due to the formation of $ANbO_3$.

Table 1. Reported values for the extinction coefficient of hexaniobate and hexatantalate ions.

pH of measurement	Species	λ_{max} (nm)	ε^a (L/mol/cm)	Reference
9.9 – 11.2	/	~233	~25 000	4
13	/	~243	~24 000	4
14	/	~248	~29 000	4
13.5	/	242	~10 900	22
10.2 – 11.5	$H_3Nb_6O_{19}^{5-}$	~235	3 200	23
10.2 – 11.5	$H_2Nb_6O_{19}^{6-}$	~232	3 000	23
10.2 – 11.5	$HNb_6O_{19}^{7-}$	~235	2 400	23
	$Nb_6O_{19}^{8-}$	~248	3 000	23
8.5	/	230	~12 500	27
12 – 14.6	$HNb_6O_{19}^{7-}$	240.5	14 300 ± 400	This work
12 – 14.6	$Nb_6O_{19}^{8-}$	247.5	15 900 ± 600	This work
12.2	$Ta_6O_{19}^{8-}$	/	3 600 at 230 nm	5
12 – 15	$Ta_6O_{19}^{8-}$	/	4 000 ± 150 at 230 nm	This work

a: Value calculated from the metal concentration, path length and absorbance published in the original articles. Absorbance values and wavelengths were determined with PlotDigitizer software.

The strong absorbance band observed for $H_xNb_6O_{19}^{x-8}$ ions varies with the pH due to the protonation or deprotonation. The strongest absorbance is observed at hydroxide concentration higher than 3 M where the cluster is fully deprotonated. Therefore, the isolation of $Nb_6O_{19}^{8-}$ under high alkaline conditions allows the direct determination of its molar absorptivity. In a prior study, Spinner and co-workers[23] reported that after 3 days and at pH ≥ 14, hexaniobate ions are transformed into the tetrameric species $Nb_4O_{12}(OH)_4^{8-}$ and $Nb_4O_{16}^{12-}$. This assumption was based on spectrophotometric measurements. We did not observe significant variations on the UV spectra over time, even after several days in solutions containing up to 9 M KOH (Fig. S1). It should be noted that hexaniobate salts can be synthesized in very basic conditions such as alkaline fusion so it would be very unlikely that the Lindqvist ion is unstable at high pH. The same group also reported extinction coefficient values for $H_xNb_6O_{19}^{x-8}$ ions largely underestimated as highlighted in Table 1. In one hand, the formation of tetrameric species in solution was never confirmed by another group but Spinner's study was mentioned in few literature reviews.[26,28,29] In the other hand, $Nb_6O_{19}^{8-}$ was observed in solutions at pH higher than 14 by multiple techniques (Raman, SAXS, NMR)[30,31,32]. Consequently, the existence of tetrameric niobates seems rather unlikely.

The strong absorbance that exhibits $Nb_6O_{19}^{8-}$ offers an easy and cheap way of titrating niobium solutions. Several UV-based methods have been developed previously for Nb(V) containing samples but they all require expensive or toxic complexing agents and none of them were applied to alkaline samples.[33,34,35,36] Moreover, these methods often contain a liquid-liquid extraction step prior to the spectrophotometric measurement. After determining precisely the extinction coefficient of $Nb_6O_{19}^{8-}$ ion, acidic samples of niobium oxalate and niobium chloride could be titrated by their dilution in 4 M KOH. In chloride media, Nb(V) forms chloro-oxo ions $[NbO_m(OH)_nCl_l]^{5-2m-n-l}$ whereas solutions of commercial $Nb(HC_2O_4)_5,nH_2O$ contains both $[NbO(C_2O_4)_3]^{3-}$ and $[NbO(H_2O)(C_2O_4)_3]^{-}$.[30,37] $[NbO_m(OH)_nCl_l]^{5-2m-n-l}$, $[NbO(C_2O_4)_3]^{3-}$ and $[NbO(H_2O)(C_2O_4)_2]^{-}$ ions are readily transformed into hexaniobate ions since (i) the strong absorbance band at 247.5 nm is observed after dilution of niobium chloride or niobium oxalate solutions in alkaline media, and (ii) the Nb contents determined by spectrophotometric titration match those determined by ICP-AES. This could open ways for new synthetic methods of hexaniobate salts under mild aqueous conditions and using commercially available materials since it is not the case for Nb_2O_5,nH_2O used in many synthesis. The method developed (dilution in 4 M KOH and UV titration) could also be useful for the determination of Nb content in hydrous niobium oxide Nb_2O_5,nH_2O which is known to be soluble in alkaline solutions[8] and used in several niobium studies.[38] Our UV-based method was also applied to industrial samples of hexaniobates since alkaline media are catching growing attention in Nb and Ta recovery processes. The Nb samples were slightly contaminated by tantalum (Nb/Ta = 80 mol/mol) but due to the

low absorbance properties of $Ta_6O_{19}^{8-}$ compared to $Nb_6O_{19}^{8-}$ ($\varepsilon_{Nb6O19}/\varepsilon_{Ta6O19}$ = 80 at 247.5 nm), the niobium concentration can still be determined by UV spectrophotometry. Thus, UV titrations of niobium can be helpful in the development of hydrometallurgical processes that aim at recovering or purifying niobium from ores.

Previous studies revealed that $Nb_6O_{19}^{8-}$ and $Ta_6O_{19}^{8-}$ clusters can be protonated. The protonation constants reported for these ions are given in Table 2. All reported data on hexaniobate ions are derived from potentiometric titrations, and due to the high value of the first protonation constant (>12.5), the authors had to extrapolate it. At an ionic strength of 3 M KCl/KOH, the value determined in the present study is in the range of the previously extrapolated values. It should be underlined that the pKa reported by Spinner[25] is about 1 log unit lower than those reported by Neuman, Etxebarria et al. and this work.

The protonation constant measured at different ionic strengths in K^+ containing media shows a decrease of this constant when the potassium concentration increases (Fig. 6). The trend is opposed to what was observed by Spinner et al. but, as explained above, their pioneer studies seem doubtful. Interactions between hexaniobate and K^+, Rb^+ or Cs^+ ions at very high pH values have been highlighted by the Nyman's group based on small-angle X-ray scattering experiments.[31,39] The authors reported the formation of the solvent-shared ion-pairs $K_8Nb_6O_{19}$ and $[K_{10}Nb_6O_{19}]^{2+}$ in 3 M potassium hydroxide solutions. In the solid state, the eight K^+ ions are associated by the cluster faces and edges through the bridging oxygens (Fig. 1).[8] It has also been proved by multinuclear NMR studies that the protonation of $Nb_6O_{19}^{8-}$, in both the solid state and solution, occurs at the bridging oxygens and not at the terminal oxygens.[40] This was also checked by our DFT computations: while the addition of one proton on a terminal oxygen leads to structures that are very difficult to stabilize, the binding of a proton on a bridging oxygen is easily realized and leads to a structure consistent with expectations. Therefore, high alkali concentration should facilitate the formation of non-protonated $Nb_6O_{19}^{8-}$ yielding a lower protonation constant.

Due to low solubility of sodium hexaniobate salts and the alkaline error in Na^+ media, the previous potentiometric studies were not performed in such media (Table 2). The low Nb concentration required by UV titration ($[Nb_6O_{19}]$ = 1 to $5*10^{-5}$ M) allowed us to investigate the protonation of $Nb_6O_{19}^{8-}$ in Na^+ media. The measurements in NaCl/NaOH media yielded lower protonation constants than in KOH/KCl media (Fig. 6). It is well-known that ion-pairing between alkali and hexaniobate ions follows the trend Cs > Rb > K > Na > Li.[3,39] Contrary to Li^+ and Na^+ media, the strong ion-pairing effect in K^+, Rb^+ and Cs^+ media allows the stabilization of protonated clusters as it is visible in the solid state. Indeed, di-protonated and mono-protonated hexaniobate salts can be synthesized with potassium, rubidium and cesium[8,41] whereas di-protonated sodium hexaniobate and protonated lithium hexaniobate have never been isolated. Thus, $H_xNb_6O_{19}^{x-8}$ ions are easier to deprotonate in Li^+ and Na^+ than in K^+, Rb^+ and Cs^+ media. This implies that proton equilibria for hexaniobate clusters should be seen as an exchange between alkali ions and protons rather than a simple proton release. Nonetheless, the stoichiometry and formation constants of the ion-pairs formed between K^+ and $HNb_6O_{19}^{7-}$ are still unknown so that the current acid-base model cannot take into account the ion-pairing effect.

Table 2. Protonation constants of hexaniobate and hexatantalate ions

i	$\log \beta_i$ for reaction $Nb_6O_{19}^{8-} + i\,H^+ = H_iNb_6O_{19}^{i-8}$			
1	13.8 ±0.2	12.6 ±0.1	13.63 ±0.04	13.4 ±0.1
2	24.68 ±0.05	23.46 ±0.15	23.55 ±0.04	/
3	/	32.85 ±0.17	32.90 ±0.07	/
	3 M KCl, T= ? 10.7≤pH≤12.4 Pot.[a]	3 M KCl 25°C 8≤pH≤12.1 Pot.[a]	3 M KCl 25°C 9.7≤pH≤13.1 Pot.[a]	3 M KCl 25°C 12≤pH≤14.5 UV-vis
Ref	24	25	26	This work
i	$\log \beta_i$ for reaction $Ta_6O_{19}^{8-} + i\,H^+ = H_iTa_6O_{19}^{i-8}$			
1	<10	12.68 ±0.1	13.89 ±0.02	11.5
2	/	23.49 ±0.2	25.91 ±0.01	20.8
3	/	32.77 ±0.25	/	/
	0.5 M KCl 25°C 10≤pH≤13 Pot.[a]	1 M KCl 25°C 8.5≤pH≤12 Pot.[a]	3 M KCl 25°C 12.4≤pH≤13 Pot.[a]	3 M KCl 25°C 10.4≤pH≤14.5 ^{17}O NMR
Ref	5	43	42	7

a: potentiometric measurements

For $H_xTa_6O_{19}^{x-8}$, no changes where observed on the UV spectra at pH ≥ 12 indicating that the tantalum cluster is fully deprotonated under these conditions. The published values on the first protonation constant of $Ta_6O_{19}^{8-}$ are largely dispersed compared to those for $Nb_6O_{19}^{8-}$ (Table 2). Our observations are in agreement with the most recent study performed by Balogh et al.[7] Knowing that a protonated hexatantalate salt has never been isolated by aqueous synthesis, the pKa values of 12.68 and 13.89, extrapolated from potentiometric measurements by Arana et al.[42] and Spinner and Kheddar[43], respectively, seem overestimated. To support this conclusion, the proton transfer was studied by DFT computations. More precisely, the thermodynamic quantities of reaction (3) were computed.

$$HNb_6O_{19\,(aq)}^{7-} + Ta_6O_{19\,(aq)}^{8-} = Nb_6O_{19\,(aq)}^{8-} + HTa_6O_{19\,(aq)}^{7-} \quad (3)$$

Interestingly, $\Delta_rG°$ = 7.1 kJ/mol is obtained (as explained in computational details, the energetic contribution to this quantity is computed at the Def2-TZVP level while the entropic contribution is computed with a smaller model). For the sake of clarity, $\Delta_rG°$ should be expressed in terms of pKa difference under the form pKa($HNb_6O_{19}^{7-}$ / $Nb_6O_{19}^{8-}$) - pKa($HTa_6O_{19}^{7-}$ / $Ta_6O_{19}^{8-}$) = 1.3. Considering the precision of the methods used, this value is in good agreement with the pKa's determined experimentally in this work and by Balogh et al. whose value is 1.9 (Table 2), thus, confirming the more difficult protonation of the hexatantalate versus the hexaniobate. These computational results are also consistent with those obtained in previous works.[7]

The effect of temperature on the protonation of $Nb_6O_{19}^{8-}$ was evaluated (Fig. 7). The protonation reaction was found

exothermic with a reaction enthalpy of $\Delta_r H$ = -95.1 kJ per mole of hexaniobate. Consequently, the non-protonated species is favored when the temperature increases. The protonation constant was shifted by almost 1 log unit between 20 °C and 40 °C highlighting the importance of this parameter during the synthesis of hexaniobate salts and for separation processes. The temperature effect could also explain the slightly higher value reported in Neuman's study which was performed at room temperature (Table 2).

The tremendous difference between the UV spectra of the isostructural ions $Nb_6O_{19}^{8-}$ and $Ta_6O_{19}^{8-}$ was investigated by DFT calculations. The UV spectra were computed for each species and are depicted in Fig. 8. A good agreement is obtained between the computed and experimental spectra as shown by the comparison between Fig. 5 and Fig. 8 (the wavelengths domain is more extended on the computed spectra than on the experimental one). Especially, the computed absorption is much lower in the case of hexatantalate from 230 nm. It should be noticed than the convoluted bands originates from several transitions; to give more insights on this aspect, the nature of the main transitions are reported in Table 3.

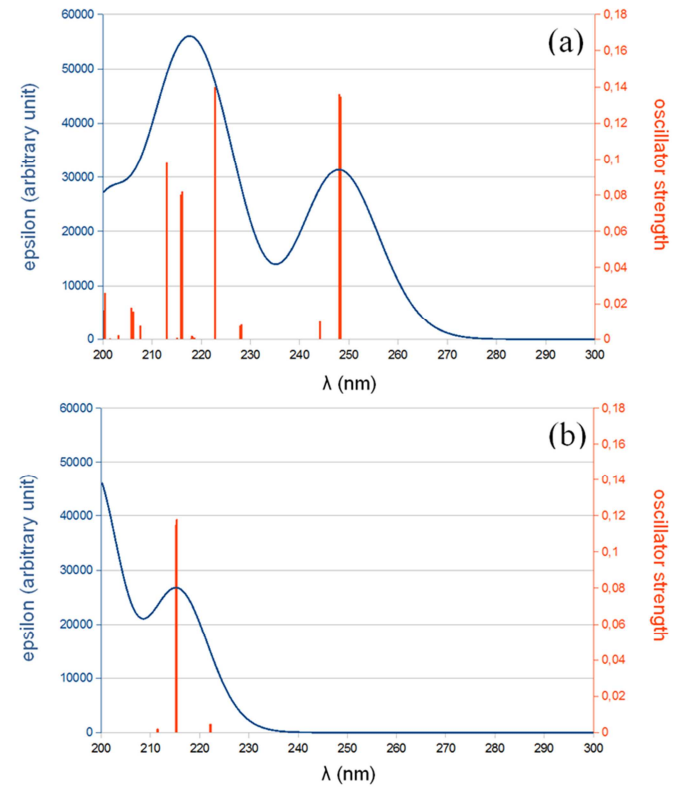

Fig. 8 Computed transitions (orange) and convoluted spectra (blue) for $Nb_6O_{19}^{8-}$ (a) and $Ta_6O_{19}^{8-}$ (b) ions. The scale is the same for both spectra.

The precise investigation of the transitions explains two important aspects of the measured spectra. First, the apparent lack of absorption of the hexatantalate is simply explained by a blue-shift of the transitions whose lowest absorption bands emerge from. Indeed, the transitions displace electron density from bridging oxygens to π* orbitals mainly localized on the metal atom. The energetic level being higher in Ta(V) than in Nb(V) (the latter is above than the former in the periodic table), the transition in consistently blue-shifted in Ta vs. Nb. Second, the effect of the protonation of hexaniobate (reported in Fig. 5) consists mainly in a blue-shift of the measured band. Once again it should be explained while considering the nature of the transition: the protonation of μ_2O (justified above) leads to a lower possibility for the electron density around those atoms to be implied in transitions, then to a blue-shift of the absorption band.

Table 3. Main electronic transitions (f > 0.03) computed for each species, oscillator strength and nature of the transition on the 200-300 nm domain.

Species	Transition wavelength (nm)	Oscillator strength	Nature of the transition
$Nb_6O_{19}^{8-}$	248.3	0.135	$n(\mu_2O) \rightarrow \pi^*(Nb\text{-}\mu_2O)$
	248.1	0.136	$n(\mu_2O) \rightarrow \pi^*(Nb\text{-}\mu_2O)$
	248.1	0.136	$n(\mu_2O) \rightarrow \pi^*(Nb\text{-}\mu_2O)$
	222.8	0.140	$n(O\ (all)) \rightarrow n(\mu_2O)$
	222.7	0.136	$n(O\ (all)) \rightarrow n(\mu_2O)$
	222.7	0.136	$n(O\ (all)) \rightarrow n(\mu_2O)$
$Ta_6O_{19}^{8-}$ [a]	215.4	0.118	$n(\mu_2O) \rightarrow \pi^*(Ta\text{-}\mu_2O)$
	215.3	0.118	$n(\mu_2O) \rightarrow \pi^*(Ta\text{-}\mu_2O)$
	215.2	0.115	$n(\mu_2O) \rightarrow \pi^*(Ta\text{-}\mu_2O)$

a: Several transitions are computed around 199 nm that justifies the general features of the convoluted spectrum for hexatantalate

Conclusions

The hexaniobate ions, $HNb_6O_{19}^{7-}$ and $Nb_6O_{19}^{8-}$, exhibit a strong absorbance band in the UV region 230-250 nm. Taking advantage of the different UV-vis properties of $Nb_6O_{19}^{8-}$ and $Ta_6O_{19}^{8-}$, a cheap and fast method was developed to determine the Nb content of both synthetic and industrial samples. For the first time, the protonation constant of $Nb_6O_{19}^{8-}$ has been determined experimentally. The nature of the electrolyte and the temperature were found to play a major role on the protonation of $Nb_6O_{19}^{8-}$ highlighting the need for further investigations on the ion-pairing between alkali ions and polyoxometalates. Due to the large uncertainties on previously reported studies, the absorbance properties and the protonation of the isostructural ions $Ta_6O_{19}^{8-}$ and $Nb_6O_{19}^{8-}$ were investigated by quantum-chemistry-based methods and corroborate the experimental findings. The UV properties of the hexaniobate ions could help to develop UV-based methods for probing the solution thermodynamics of Nb(V) in alkaline media. We are currently exploiting the spectral properties of $H_xNb_6O_{19}^{x-8}$ and $H_xTa_6O_{19}^{x-8}$ to study alkaline solutions of Nb(V) and Ta(V) by capillary electrophoresis.

Acknowledgements

This work was granted access to the HPC resources of CINES under the allocation 2014086933 made by GENCI (Grand

Equipement National de Calcul Intensif). We also thank the CRI (Centre de Ressources Informatiques) of the Université de Lille for providing computing time for part of the theoretical calculations. The experimental part of this work was financed by Eramet Research (France).

Notes and references

[a] *PSL Research University, Chimie ParisTech - CNRS, Institut de Recherche de Chimie Paris, 11 rue Pierre et Marie Curie, 75005 Paris, France*. Email : gauthier.deblonde@chimie-paris.org

[b] *Eramet Research, Hydrometallurgy department, F-78193 Trappes, France*.

[c] *LASIR (UMR CNRS 8516) – Université de Lille - Sciences et Technologies, 59655 Villeneuve d'Ascq, France*.

† Electronic Supplementary Information (ESI) available: See DOI: 10.1039/b000000x/

1 Z. Zhu and C. Y. Cheng, *Hydrometallurgy*, 2011, **107**, 1–12.
2 X. Wang, S. Zheng, H. Xu and Y. Zhang, *Hydrometallurgy*, 2009, **98**, 219–223.
3 M. Nyman, *Dalton Trans.*, 2011, **40**, 8049.
4 G. Jander and D. Ertel, *J. Inorg. Nucl. Chem.*, 1960, **14**, 71–76.
5 H. W. Nelson and S. Tobias, *Inorg. Chem.*, 1963, **2**, 985–992.
6 R. t Shannon, *Acta Crystallogr. A*, 1976, **32**, 751–767.
7 E. Balogh, T. M. Anderson, J. R. Rustad, M. Nyman and W. H. Casey, *Inorg. Chem.*, 2007, **46**, 7032–7039.
8 M. Nyman, T. M. Alam, F. Bonhomme, M. A. Rodriguez, C. S. Frazer and M. E. Welk, *J. Clust. Sci.*, 2006, **17**, 197–219.
9 P. Gans, A. Sabatini and A. Vacca, *Talanta*, 1996, 1739–1753.
10 M. Sturzbecher-Hoehne, C. Ng Pak Leung, A. D'Aléo, B. Kullgren, A.-L. Prigent, D. K. Shuh, K. N. Raymond and R. J. Abergel, *Dalton Trans.*, 2011, **40**, 8340.
11 G. J-P. Deblonde, M. Sturzbecher-Hoehne and R. J. Abergel, *Inorg. Chem.*, 2013, **52**, 8805–8811.
12 M. Sturzbecher-Hoehne, G. J-P. Deblonde and R. J. Abergel, *Radiochim. Acta*, 2013, **101**, 359–366.
13 F. H. Sweeton, R. E. Mesmer and C. F. Baes Jr, *J. Solut. Chem.*, 1974, **3**, 191–214.
14 I. Kron, S. L. Marshall, P. M. May, G. Hefter and E. Königsberger, *Monatshefte Für Chem.*, 1995, **126**, 819–837.
15 J. P. Perdew, M. Burke and M. Ernzerhof, *Phys. Rev. Lett.*, 1996, **77**, 3865–3868.
16 C. Adamo and V. Barone, *J. Chem. Phys.*, 1999, **110**, 6158.
17 Gaussian 09, Revision D.01, Frisch, M. J.; Trucks, G. W.; Schlegel, H. B.; Scuseria, G. E.; Robb, M. A.; Cheeseman, J. R.; Scalmani, G.; Barone, V.; Mennucci, B.; Petersson, G. A.; Nakatsuji, H.; Caricato, M.; Li, X.; Hratchian, H. P.; Izmaylov, A. F.; Bloino, J.; Zheng, G.; Sonnenberg, J. L.; Hada, M.; Ehara, M.; Toyota, K.; Fukuda, R.; Hasegawa, J.; Ishida, M.; Nakajima, T.; Honda, Y.; Kitao, O.; Nakai, H.; Vreven, T.; Montgomery, J. A., Jr.; Peralta, J. E.; Ogliaro, F.; Bearpark, M.; Heyd, J. J.; Brothers, E.; Kudin, K. N.; Staroverov, V. N.; Kobayashi, R.; Normand, J.; Raghavachari, K.; Rendell, A.; Burant, J. C.; Iyengar, S. S.; Tomasi, J.; Cossi, M.; Rega, N.; Millam, M. J.; Klene, M.; Knox, J. E.; Cross, J. B.; Bakken, V.; Adamo, C.; Jaramillo, J.; Gomperts, R.; Stratmann, R. E.; Yazyev, O.; Austin, A. J.; Cammi, R.; Pomelli, C.; Ochterski, J. W.; Martin, R. L.; Morokuma, K.; Zakrzewski, V. G.; Voth, G. A.; Salvador, P.; Dannenberg, J. J.; Dapprich, S.; Daniels, A. D.; Farkas, Ö.; Foresman, J. B.; Ortiz, J. V.; Cioslowski, J.; Fox, D. J. Gaussian, Inc., Wallingford CT, 2009.
18 T. H. Dunning Jr and P. J. Hay, in *Modern Theoritical Chemistry*, ed. H. F. Schafer, New-York, III., 1977, vol. 3, pp. 1–28.
19 M. Dolg, H. Stoll, H. Preuss and R. M. Pitzer, *J. Chem. Phys.*, 1993, **97**, 5852.
20 F. Weigend and R. Ahlrichs, *Phys. Chem. Chem. Phys.*, 2005, **7**, 3297–3305.
21 J. Tomasi, B. Mennucci and R. Cammi, *Chem. Rev.*, 2005, **105**, 2999–3094.
22 G. I. Gridchina, *Russ. J. Inorg. Chem.*, 1963, **8**, 322–326.
23 A. Goiffon, R. Granger, C. Bockel and B. Spinner, *Rev. Chim. Minérale*, 1973, **10**, 487.
24 G. Neumann, *Acta Chem. Scand.*, 1964, **18**, 278–280.
25 B. Spinner, *Rev. Chim. Minérale*, 1968, 839–868.
26 N. Etxebarria, L. A. Fernandez and J. M. Madariaga, *J. Chem. Soc. Dalton Trans.*, 1994, 3055.
27 J. R. Black, M. Nyman and W. H. Casey, *J. Am. Chem. Soc.*, 2006, **128**, 14712–14720.
28 F. Sahureka, R. C. Burns and E. I. von Nagy-Felsobuki, *Inorganica Chim. Acta*, 2003, **351**, 69–78.
29 G. M. Rozantsev, O. I. Dotsenko and G. V. Taradina, 2000, **26**, 264–270.
30 J.-M. Jehng and I. E. Wachs, *J. Raman Spectrosc.*, 1991, **22**, 83–89.
31 M. R. Antonio, M. Nyman and T. M. Anderson, *Angew. Chem. Int. Ed.*, 2009, **48**, 6136–6140.
32 G. K. Goh, F. F. Lange, S. M. Haile and C. G. Levi, *J. Mater. Res.*, 2003, **18**, 338–345.
33 K. Patel, S. K. Menon and Y. K. Agrawal, *Microchem. J.*, 1996, **53**, 158–163.
34 A. K. Chhakkar and L. R. Kakkar, *Fresenius J. Anal. Chem.*, 1995, **351**, 720–723.
35 N. Agnihotri, R. Kamal and J. R. Mehta, *Ann. Chim.*, 2006, **96**, 479–485.
36 N. Agnihotri and J. R. Mehta, *Chem. Anal.*, 2005, **50**, 429.
37 V. Pershina, *Radiochim. Acta*, 1998, **80**, 75–84.
38 K. Nakajima, Y. Baba, R. Noma, M. Kitano, J. N. Kondo, S. Hayashi and M. Hara, *J. Am. Chem. Soc.*, 2011, **133**, 4224–4227.
39 M. K. Kinnan, W. R. Creasy, L. B. Fullmer, H. L. Schreuder-Gibson and M. Nyman, *Eur. J. Inorg. Chem.*, 2014, **2014**, 2361–2367.
40 T. M. Alam, M. Nyman, B. R. Cherry, J. M. Segall and L. E. Lybarger, *J. Am. Chem. Soc.*, 2004, **126**, 5610–5620.
41 I. Santos, L. H. Loureiro, M. F. P. Silva and A. Cavaleiro, *Polyhedron*, 2002, **21**, 2009–2015.
42 G. Arana, N. Etxebarria, L. A. Fernandez and J. M. Madariaga, *J. Solut. Chem.*, 1995, **24**, 611–622.
43 B. Spinner and N. Kheddar, *Comptes Rendus Académie Sci. Sér. C*, 1969, **t. 269**, 1108–1111.